Dalton Transactions

ROYAL SOCIETY OF CHEMISTRY

PAPER

View Article Online
View Journal | View Issue

Cite this: *Dalton Trans.*, 2020, **49**, 8504

High-valent osmium iminoxolene complexes†

Jacqueline Gianino, Alexander N. Erickson, Sean J. Markovitz and Seth N. Brown *

Received 13th May 2020,
Accepted 5th June 2020

DOI: 10.1039/d0dt01735c

rsc.li/dalton

2-(Arylamino)-4,6-di-*tert*-butylphenols containing 4-substituted phenyl groups ($^{R}apH_2$) react with oxobis(ethylene glycolato)osmium(VI) in acetone to give square pyramidal bis(amidophenoxide)oxoosmium(VI) complexes. A mono-amidophenoxide complex is observed as an intermediate in these reactions. Reactions in dichloromethane yield the diolate $(^{H}ap)_2Os(OCH_2CH_2O)$. Both the glycolate and oxo complex are converted to the corresponding *cis*-dichloride complex on treatment with chlorotrimethylsilane. The novel bis(aminophenol) ligand $EganH_4$, containing an ethylene glycol dianthranilate bridge, forms the chelated bis(amidophenoxide) complex (Egan)OsO, where the two nitrogen atoms of the tetradentate ligand bind in the trans positions of the square pyramid. Structural and spectroscopic features of the complexes are described well by an osmium(VI)-amidophenoxide formulation, with the amount of π donation from ligand to metal increasing markedly as the co-ligands change from oxo to diolate to dichloride. In the oxo-bis(amidophenoxides), the symmetry of the ligand π orbitals results in only one effective π donor interaction, splitting the energy of the two osmium-oxo π* orbitals and rendering the osmium-oxo bonding appreciably anisotropic.

Introduction

2-Amidophenoxides, like their isoelectronic analogues catecholates and diamidobenzenes, are celebrated for their ability to undergo changes in oxidation state in their metal complexes.[1] The accessibility of the amidophenoxide, iminosemiquinone, and iminoquinone oxidation states arises from the presence of an orbital in the iminoquinone (called the redox-active orbital or RAO, Fig. 1) at a moderate energy, so that it can be occupied by two, one, or zero electrons. In addition to contributing to redox activity, the moderate energy of this orbital, combined with its substantial density on the ligating oxygen and nitrogen atoms, make this orbital a strong π donor. For example, the strength of the molybdenum-amidophenoxide π interaction has been estimated at 40 kcal mol^{-1}.[2]

Because the metal orbitals become progressively lower in energy as one goes to the right across the d block, early transition metals have d orbitals that are higher in energy than the iminoxolene RAO[3] and late transition metals have d orbitals that are lower in energy than the iminoxolene RAO.[4] Thus, the covalency of the metal-iminoxolene π interaction is expected to be maximized near the center of the periodic table, where the energies of the metal and ligand orbitals are most closely matched. In particular, iminoxolene complexes of ruthenium and osmium appear to be highly covalent, with the π bonding orbitals having slightly more metal than ligand character for ruthenium and slightly more ligand than metal character for osmium.[5]

The energy of the metal dπ orbitals depends not only on the identity of the metal but also on the nature of the ancillary ligands, as π donor ligands can raise the energies of the dπ orbitals and π acceptor ligands can lower their energies. This effect has been observed octahedral d^0 *cis*-oxo-bis(amidophenoxide) complexes of molybdenum[6] and rhenium.[7] The amidophenoxide *cis* to the oxo group must donate to a dπ orbital that is already π* to the oxo group and is observed to be an ineffec-

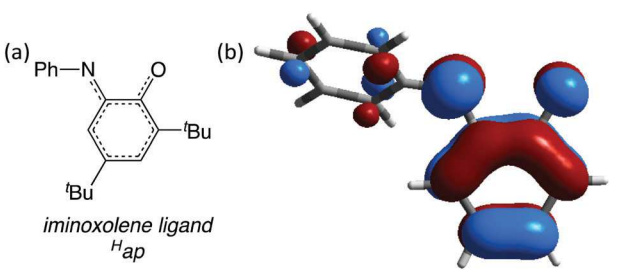

Fig. 1 (a) Connectivity of the iminoxolene ligand ^{H}ap. (b) Iminoxolene redox-active orbital or RAO. This corresponds to the LUMO of neutral iminoquinone ^{H}ap, the SOMO of the monoanionic iminosemiquinonate $^{H}ap^{-}$, and the HOMO of dianionic amidophenoxide $^{H}ap^{2-}$.

Department of Chemistry and Biochemistry, 251 Nieuwland Science Hall, University of Notre Dame, Notre Dame, IN 46556-5670, USA.
E-mail: Seth.N.Brown.114@nd.edu; Fax: +1 01574 631 6652; Tel: +1 01 574 631 4659

† Electronic supplementary information (ESI) available: Spectroscopic, structural and electrochemical data and computational details. CCDC 2003363–2003368. For ESI and crystallographic data in CIF or other electronic format see DOI: 10.1039/d0dt01735c

tive π donor, while the other amidophenoxide can donate into a d orbital that is of δ symmetry with respect to the metal-oxo bond and is observed to be a strong π donor.

Here we describe the preparation and characterization of oxoosmium bis(iminoxolene) complexes and examine the competition for π bonding between the oxo and iminoxolene ligands. As in the compounds of groups 6 and 7, the oxo ligand in the group 8 compound dominates the π bonding, so the complexes are well described as oxoosmium(VI) amidophenoxide complexes. As divalent O^{2-} is replaced by ethylene glycolate or two chlorides, the decreasing π donation of the ancillary ligands is compensated by increasing donation from the amidophenoxide ligands. Spectroscopic and computational studies indicate that there is still some π donation from the amidophenoxide ligands in $(^{H}ap)_2OsO$, and the symmetry constraints of the orbitals lead to a noticeable anisotropy in the π bonding to the oxo ligand.

Experimental section

General procedures

All procedures were carried out on the benchtop without precautions to exclude air or moisture. 2-(Arylamino)-4,6-di-*tert*-butylphenols containing 4-substituted aryl groups $^{H}apH_2$,[8] $^{MeO}apH_2$[9] and $^{CF3}apH_2$[10] were prepared by published procedures. $OsO(OCH_2CH_2O)_2$ was prepared as described by Griffith.[11] Deuterated solvents were obtained from Cambridge Isotope Laboratories. All other reagents were commercially available and used without further purification. NMR spectra were measured on a Bruker Avance DPX-400 or −500 spectrometer. Chemical shifts for ^{1}H and ^{13}C are reported in ppm downfield of TMS, with spectra referenced using the chemical shifts of the solvent residuals, while ^{19}F chemical shifts are reported in ppm downfield of internal $CFCl_3$. Infrared spectra were recorded on a Jasco 6300 FT-IR spectrometer as solids using an ATR plate. UV-visible spectra were measured as CH_2Cl_2 solutions in a 1 cm quartz cell on a ThermoFisher Evolution Array diode array spectrophotometer or a Hitachi U-2910 spectrophotometer. UV-vis-NIR spectra were recorded on a JASCO V-670 spectrophotometer. Elemental analyses were performed by M–H–W Laboratories (Phoenix, AZ, USA).

Syntheses

Oxobis(2-(phenylimino)-4,6-di-*tert*-butylphenoxo)osmium(VI), $(^{H}ap)_2OsO$. Into a 125 mL Erlenmeyer flask is weighed 0.6004 g $OsO(OCH_2CH_2O)_2$ (1.840 mmol) and 1.1540 g $^{H}apH_2$ (3.893 mmol, 2.11 equiv.). To the flask is added 30 mL acetone and a stirbar. The flask is covered with parafilm and the reaction mixture is stirred 22 h at room temperature. The mixture is suction filtered and the solid washed thoroughly with 2 × 10 mL acetone, then 2 × 10 mL dichloromethane, then air-dried 30 min to yield 1.2570 g $(^{H}ap)_2OsO$ (86%). ^{1}H NMR (CD_2Cl_2): δ 0.95, 1.20 (s, 18H each, ^{t}Bu), 6.62, 6.73 (d, 2 Hz, 2H each, ap 3,5-H), 7.33 (tt, 7, 1 Hz, 2H, *p*-Ph), 7.36 (d, 7 Hz, 4H, *o*-Ph), 7.50, 7.63 (sl br t, 7 Hz, 2H each, *m*-Ph). The compound was not sufficiently soluble for $^{13}C\{^{1}H\}$ NMR analysis. IR (cm^{-1}): 2949 (m), 2902 (w), 2867 (w), 1591 (m), 1568 (m), 1479 (m), 1457 (m), 1404 (s), 1360 (s), 1314 (m), 1261 (m), 1238 (m), 1219 (m), 1201 (m), 1162 (w), 1109 (w), 1074 (m), 1030 (m), 996 (s), 967 (w), 938 (s), 906 (vs, $\nu_{Os=O}$), 896 (s), 861 (s), 827 (m), 768 (m), 761 (s), 746 (w), 726 (vs), 698 (s), 689 (s). UV-vis (CH_2Cl_2): λ_{max} 580 nm (sh, ε = 4400 L mol^{-1} cm^{-1}), 458 (11 100), 364 (17 200), 286 (16 300). Anal. Calcd for $C_{40}H_{50}N_2O_3Os$: C, 60.27; H, 6.32; N, 3.51. Found: C, 60.12; H, 6.44; N, 3.41.

Oxobis(2-(4-methoxyphenylimino)-4,6-di-*tert*-butylphenoxo)osmium(VI), $(^{MeO}ap)_2OsO$. The compound was prepared analogously to the phenyl derivative using 0.2731 g $OsO(OCH_2CH_2O)_2$ (0.837 mmol) and 0.5753 g $^{MeO}apH_2$ (1.757 mmol, 2.10 eq.) to yield 0.3392 g $(^{MeO}ap)_2OsO$ (47%). The NMR spectra in CD_2Cl_2 indicate that the compound exists as a 85 : 15 mixture of geometric isomers at room temperature. ^{1}H NMR (CD_2Cl_2): major isomer: δ 0.99, 1.21 (s, 18H each, ^{t}Bu), 3.92 (s, 6H, OCH_3), 6.63, 6.77 (d, 2 Hz, 2H each, ap 3,5-H), 7.03 (d, 8 Hz, 2H, $C_6H_4OCH_3$, *ortho* to OCH_3), 7.12 (d, 8 Hz, 2H, $C_6H_4OCH_3$ *ortho* to OCH_3), 7.28 (m, 4H, $C_6H_4OCH_3$ *ortho* to N). Minor isomer: δ 0.93, 1.25 (s, 18H each, ^{t}Bu), 3.71 (s, 6H, OCH_3), 6.44 (v br, 4H, $C_6H_4OCH_3$ *ortho* to N), 7.12 (d, 2H, ap 3,5-H), 7.21 (br d, 8 Hz, 4H, $C_6H_4OCH_3$ *ortho* to OCH_3), 7.28 (d, 2H, ap 3,5-H). $^{13}C\{^{1}H\}$ NMR (CD_2Cl_2, major isomer only): δ 29.61, 32.11 ($C(CH_3)_3$), 34.76, 34.82 ($C(CH_3)_3$), 56.25 (OCH_3), 112.11, 114.83, 115.38, 120.64, 129.16, 131.57, 135.75, 141.70, 144.83, 145.89, 149.64, 159.85 (ap *OC*). IR (cm^{-1}): 2955 (m), 2903 (w), 2867 (w), 2833 (w), 1602 (m), 1572 (m), 1502 (s), 1464 (m), 1439 (m), 1405 (m), 1359 (m), 1300 (m), 1239 (s), 1220 (s), 1179 (m), 1170 (m), 1105 (m), 1043 (s), 1029 (m), 1009 (w), 999 (s), 956 (w), 945 (m), 922 (m), 906 (vs, $\nu_{Os=O}$), 861 (m), 839 (m), 828 (w), 822 (w), 808 (w), 792 (w), 760 (m), 745 (w), 734 (s), 715 (m), 687 (w), 679 (w), 654 (m). UV-vis (CH_2Cl_2): λ_{max} 598 nm (sh, ε = 4200 L mol^{-1} cm^{-1}), 465 (11 600), 367 (19 500), 283 (17 300). Anal. Calcd for $C_{42}H_{54}N_2O_5Os$: C, 58.85; H, 6.35; N, 3.27. Found: C, 58.89; H, 6.16; N, 3.25.

Oxobis(2-(4-trifluoromethylphenylimino)-4,6-di-*tert*-butylphenoxo)osmium(VI), $(^{CF3}ap)_2OsO$. Into a 20 mL screw-cap vial in the air are added 0.2577 g $OsO(OCH_2CH_2O)_2$ (0.789 mmol), 0.5794 g $^{CF3}apH_2$ (1.59 mmol, 2.01 eq.), chloroform (10 mL) and a stirbar. The vial is capped securely and the reaction mixture is stirred 6 d at room temperature. The dark purple mixture is suction filtered and the solid washed thoroughly with 3 mL chloroform and 3 × 10 mL ether, then air-dried 30 min to yield 0.5320 g crude $(^{CF3}ap)_2OsO$. The material is purified by Soxhlet extraction for 3 d into 25 mL $CHCl_3$. Cooling the extract to room temperature and suction filtering the precipitated red-brown solid, washing the solid with 2 × 10 mL Et_2O, and air-drying 30 min affords 0.4072 g pure $(^{CF3}ap)_2OsO$ (55%). ^{1}H NMR (CD_2Cl_2): δ 0.94, 1.21 (s, 18H each, ^{t}Bu), 6.67, 6.74 (d, 2 Hz, 2H each, ap 3,5-H), 7.50, 7.52 (sl br d, 8 Hz, 2H each, *meta* to CF_3), 7.78, 7.92 (sl br d, 8 Hz, 2H each, *ortho* to CF_3). $^{19}F\{^{1}H\}$ NMR (CD_2Cl_2): δ −62.47 (s). The compound is not sufficiently soluble for $^{13}C\{^{1}H\}$ NMR analysis. IR (cm^{-1}): 2963 (m), 2912 (w), 2871 (w), 1611 (m), 1596 (w),

1571 (w), 1480 (m), 1467 (w), 1402 (s), 1362 (m), 1320 (vs), 1264 (m), 1238 (w), 1218 (m), 1201 (w), 1177 (m), 1159 (s), 1126 (vs), 1104 (s), 1065 (vs), 1029 (m), 1016 (s), 999 (s), 971 (w), 960 (w), 934 (s), 904 (vs, $\nu_{Os=O}$), 863 (m), 849 (s), 836 (w), 825 (m), 781 (w), 759 (m), 750 (m), 741 (m), 720 (s), 695 (m), 654 (s). UV-vis (CH_2Cl_2): λ_{max} 605 nm (sh, ε = 4300 L mol^{-1} cm^{-1}), 465 (9800), 371 (13 400). Anal. Calcd for $C_{42}H_{48}F_6N_2O_3Os$: C, 54.06; H, 5.19; N, 3.00. Found: C, 54.31; H, 4.99; N, 3.05.

2-(4-(Methylthio)phenylamino)-4,6-di-*tert*-butylphenol, ^{MeS}apH$_2$. Into a 25 mL Erlenmeyer flask in the air is weighed 2.018 g 4-methylthioaniline (0.0145 mol) and 3.223 g 3,5-di-*tert*-butylcatechol (0.0145 mmol). To the flask is added 25 mL hexanes and a stirbar. The reaction mixture is stirred for 5 minutes, then 152 μL (0.0011 mol, 0.075 equiv.) Et_3N is added. The flask is covered with parafilm and the reaction mixture is stirred 24 h at room temperature. The mixture is suction filtered and the solid washed with 2 × 15 mL hexanes, then air-dried 30 min to yield 4.3283 g ^{MeS}apH$_2$ (87%). ^{1}H NMR (C_6D_6): δ 1.26, 1.62 (s, 9H each, ^{t}Bu), 2.04 (s, 3H, SC*H*$_3$), 4.04 (s, 1H, N*H*), 6.24 (s, 1H, O*H*), 6.36 (d, 8 Hz, 2H, C$_6$*H*$_4$SCH$_3$ *ortho* to N), 6.94 (d, 2 Hz, 1H, ap 3- or 5-H), 7.10 (d, 8 Hz, 2H, C$_6$*H*$_4$SCH$_3$ *ortho* to SCH$_3$), 7.43 (d, 2 Hz, 1H, ap 3- or 5-H). ^{13}C{^{1}H} NMR (C_6D_6): δ 17.81 (S*C*H$_3$), 29.70, 31.65 (C(*C*H$_3$)$_3$), 34.37, 35.23 (*C*(CH$_3$)$_3$), 116.06, 121.77, 122.01, 128.37, 130.61, 135.56, 142.34, 145.43, 149.82 (one carbon obscured by solvent peak). IR (cm^{-1}): 3430 (w, ν_{OH}), 3352 (m, ν_{NH}), 2999 (w), 2963 (m), 2915 (w), 2864 (w), 1653 (w), 1604 (m), 1559 (w), 1540 (w), 1507 (m), 1496 (s), 1483 (s), 1457 (m), 1442 (s), 1412 (m), 1388 (m), 1363 (m), 1340 (w), 1308 (s), 1282 (w), 1265 (m), 1237 (s), 1219 (s), 1201 (s), 1185 (m), 1159 (m), 1121 (w), 1095 (m), 1025 (w), 1009 (w), 890 (m), 844 (w), 812 (vs), 767 (s), 732 (w), 713 (m), 657 (m). Anal. Calcd for $C_{21}H_{29}NOS$: C, 73.42; H, 8.51; N, 4.08. Found: C, 73.67; H, 8.38; N, 4.00.

Oxobis(2-(4-methythiophenylimino)-4,6-di-*tert*-butylphenoxo) osmium(VI), (^{MeS}ap)$_2$OsO. The compound was prepared analogously to the phenyl derivative using 0.3042 g OsO(OCH$_2$CH$_2$O)$_2$ (0.932 mmol) and 0.6114 g ^{MeS}apH$_2$ (1.780 mmol, 1.91 equiv.). After filtration and washing with acetone, the crude solid is dissolved in 30 mL CH_2Cl_2 and suction filtered to remove insoluble impurities. Evaporation of the solvent from the filtrate yields 0.2650 g (^{MeS}ap)$_2$OsO (32%). NMR spectra in CD_2Cl_2 indicate a 85 : 15 mixture of isomers; only peaks due to the major isomer are listed. ^{1}H NMR (CD_2Cl_2): δ 1.00, 1.22 (s, 18H each, ^{t}Bu), 2.62 (s, 6H, SC*H*$_3$), 6.65, 6.80 (d, 2 Hz, 2H each, ap 3,5-H), 7.29 (m, 4H, C$_6$*H*$_4$SCH$_3$ *ortho* to SCH$_3$), 7.37 (d, 8 Hz, 2H, C$_6$*H*$_4$SCH$_3$, *ortho* to N), 7.49 (d, 8 Hz, 2H, C$_6$*H*$_4$SCH$_3$ *ortho* to N). ^{13}C{^{1}H} NMR (CD_2Cl_2): δ 15.90 (S*C*H$_3$), 29.21, 31.70 (C(*C*H$_3$)$_3$), 34.34, 34.44 (*C*(CH$_3$)$_3$), 111.71, 120.53, 127.01, 127.45, 127.95, 130.17, 135.56, 138.63, 145.38, 145.72, 148.71, 168.14 (ap O*C*). IR (cm^{-1}): 2970 (m), 2962 (m), 2902 (w), 2869 (w), 1684 (w), 1653 (w), 1507 (m), 1488 (m), 1457 (m), 1404 (m), 1399 (m), 1361 (m), 1317 (w), 1301 (w), 1263 (m), 1220 (m), 1202 (m), 1164 (m), 1106 (w), 1089 (m), 1029 (s), 1012 (m), 999 (s), 948 (w), 926 (m), 906 (vs, $\nu_{Os=O}$), 862 (s), 836 (m), 814 (w), 765 (m), 757 (w), 741 (s), 728 (w), 714 (w), 698 (m), 669 (m), 654 (m). UV-vis (CH_2Cl_2): λ_{max} 600 nm (sh, ε = 4000 L mol^{-1} cm^{-1}), 469 (11 200), 374 (18 700), 285 (sh, 21 400), 265 (31 100). Anal. Calcd for $C_{42}H_{54}N_2O_3OsS_2$: C, 56.73; H, 6.12; N, 3.15. Found: C, 57.80; H, 6.49; N, 3.64.

Bis(2-(phenylimino)-4,6-di-*tert*-butylphenoxo)dichloroosmium(VI), (^{H}ap)$_2$OsCl$_2$

Method A. In the drybox, a solution of 0.0667 g PCl_5 (0.32 mmol, 1.02 eq.) in 25 mL $CHCl_3$ is added to a 100 mL round bottom flask containing 0.2514 g (^{H}ap)$_2$OsO (0.315 mmol). The solution immediately turns dark purple. After 15 min, the solution is exposed to the air, washed with 2 × 50 mL H_2O, dried over $MgSO_4$, and the solvent removed on a rotary evaporator. The dark residue is slurried in pentane, suction filtered, and washed with 2 × 1 mL pentane. The solid is dried for 20 min, furnishing 0.1290 g (^{H}ap)$_2$OsCl$_2$ (48%).

Method B. To a 20 mL scintillation vial in the drybox is added 0.3789 g (^{H}ap)$_2$OsO (0.475 mmol), 12 mL C_6H_6, 242 μL (CH$_3$)$_3$SiCl (1.91 mmol, 4.01 eq.) and a stirbar. The vial is capped and taken out of the drybox and heated, with stirring, for 3 d in a 70 °C oil bath. After allowing the reaction mixture to stand at room temperature overnight, the vial is opened and the solution decanted. The solid is washed with 5 × 1 mL pentane and dried for 20 minutes to give 0.2578 g (^{H}ap)$_2$OsCl$_2$ (64%). ^{1}H NMR (CD_2Cl_2): δ 1.56 (s, 18H, ^{t}Bu), 1.21 (s, 18H, ^{t}Bu), 6.09 (br s, 2H, *o*- or *m*-Ph), 6.61, 6.83 (s, 2H each, ap 3,5-H), 7.12 (t, 7 Hz, 2H, *p*-Ph), 7.14 (br s, 2H, *o*- or *m*-Ph), 7.36 (br s, 2H, *o*- or *m*-Ph), 7.54 (br s, 2H, *o*- or *m*-Ph). ^{13}C{^{1}H} NMR (CD_2Cl_2): δ 30.27, 30.93 (C(*C*H$_3$)$_3$), 34.96, 35.41 (*C*(CH$_3$)$_3$), 109.53, 123.76 (br), 125.19 (br), 127.54 (br), 128.56 (br), 129.58, 132.25, 143.21, 155.26 (2C), 172.05, 205.37 (*C*O). IR (cm^{-1}): 3085 (w), 3045 (w), 2952 (m), 2903 (m), 2867 (m), 1623 (w), 1585 (w), 1558 (w), 1531 (m), 1506 (w), 1485 (w), 1479 (m), 1463 (w), 1456 (m), 1441 (m), 1417 (w), 1394 (w), 1389 (w), 1373 (w), 1362 (s), 1324 (w), 1305 (w), 1294 (w), 1282 (w), 1261 (s), 1233 (m), 1202 (m), 1175 (m), 1165 (s), 1120 (w), 1105 (m), 1086 (m), 1073 (m), 1025 (m), 1013 (w), 999 (m), 962 (w), 952 (w), 933 (m), 925 (m), 909 (s), 864 (m), 839 (w), 828 (m), 821 (m), 781 (m), 769 (m), 742 (s), 734 (s), 707 (s), 691 (s), 668 (s), 651 (w). UV-Vis-NIR (CH_2Cl_2): λ_{max} 1565 nm (ε = 1000 L mol^{-1} cm^{-1}), 703 (5600), 540 (31 000), 408 (9500), 343 (8500), 295 (12 500). The analytical sample was recrystallized from dichloromethane/hexane. Anal. Calcd for $C_{40}H_{50}Cl_2N_2O_2Os{\cdot}CH_2Cl_2$: C, 52.56; H, 5.59; N, 2.99. Found: C, 52.26; H, 5.65; N, 2.97.

Bis(2-(phenylimino)-4,6-di-*tert*-butylphenoxo)(ethyleneglycolato)osmium(VI), (^{H}ap)$_2$Os(OCH$_2$CH$_2$O). To a 50 mL Erlenmeyer flask are added OsO(OCH$_2$CH$_2$O)$_2$ (273.1 mg, 0.837 mmol), ^{H}apH$_2$ (444.3 mg, 1.495 mmol), 20 mL dichloromethane, and a stirbar. The flask is sealed with parafilm and the reaction mixture is stirred 40 h at room temperature. The reaction mixture is then filtered through a plug of silica gel, washing with dichloromethane to remove a brown impurity, followed by 1 : 1 ethyl acetate/hexane to elute the dark purple band of the glycolate complex. After evaporating the solvent, the residue is slurried in 4 mL hexane, suction filtered, washed with 2 × 2 mL hexane, and air-dried to yield 112.9 mg (^{H}ap)$_2$Os(OCH$_2$CH$_2$O) (18%). ^{1}H NMR (CD_2Cl_2, −83 °C; only

major isomer listed): δ 0.92, 1.18 (s, 18H each, ^{t}Bu), 5.39, 5.59 (m, 2H each, OC*HH*′C*HH*′O), 7.06, 7.08 (d, 2 Hz, 2H each, ap 3,5-H), 7.27 (d, 8 Hz, 2H, Ph), 7.43 (t, 7 Hz, 2H, Ph), 7.52 (m, 6H, Ph). IR (cm^{-1}): 3069 (w), 2952 (s), 2909 (m), 2866 (m), 2813 (m), 1742 (w), 1679 (w), 1665 (w), 1590 (m), 1549 (m), 1486 (m), 1451 (m), 1388 (m), 1361 (s), 1307 (m), 1254 (s), 1231 (s), 1201 (s), 1176 (s), 1164 (s), 1112 (w), 1073 (w), 1025 (s), 1003 (m), 907 (s), 862 (s), 825 (w), 768 (s), 743 (s), 728 (w), 707 (s), 689 (s). UV-Vis-NIR: λ_{max} 1330 nm (sh, ε = 260 L mol^{-1} cm^{-1}), 708 (3800), 531 (16 000), 417 (5600). Anal. Calcd for $C_{42}H_{54}N_2O_4Os$: C, 59.97; H, 6.47; N, 3.33. Found: C, 59.29; H, 6.62; N, 3.09.

Oxo(pinacolato)(2-(phenylimino)-4,6-di-*tert*-butylphenoxo) osmium(VI), (^{H}ap)OsO(pin). To a solution of osmium tetroxide (0.1553 g, 0.607 mmol) in CH_2Cl_2 (10 mL) is added 72 μL 2,3-dimethyl-2-butene (51 mg, 0.61 mmol). After allowing the mixture to stand for 5 min, 0.1801 g 2-(phenylamino)-4,6-di-*tert*-butylphenol (^{H}apH_2, 0.606 mmol) is added. The mixture is stirred in a sealed vial for 3 d, the volatiles removed on the rotary evaporator, and the residue triturated with methanol (10 mL). After the mixture is allowed to stand 20 min in a −20 °C freezer, it is suction filtered and the precipitate washed with 7 mL methanol. After air-drying, the yield of (^{H}ap)OsO(pin) is 0.3204 g (86%). ^{1}H NMR (CD_2Cl_2): δ 1.03, 1.11, 1.25, 1.46 (s, 3H each, pinacolate CH_3), 1.21, 1.50 (s, 9H each, ^{t}Bu), 6.58, 6.85 (d, 2 Hz, 1H each, ap 3,5-H), 7.13, 7.23, 7.50, 7.56 (br, 1H each, Ph *o*- and *m*-H), 7.34 (t, 7.5 Hz, 1H, Ph *p*-H). ^{13}C{^{1}H} NMR (CD_2Cl_2): δ 24.38, 24.75, 25.03, 25.90 (pinacol *C*H$_3$), 30.18, 32.07 (C[*C*H$_3$]$_3$), 34.77, 35.45 (*C*[CH$_3$]$_3$), 93.65, 95.60 (pinacol O*C*), 111.21, 120.44, 127.94 (br), 128.28, 129.02 (br), 129.43 (br, 2C), 136.32, 145.27, 148.39, 151.76, 165.70 (ap O*C*). IR (cm^{-1}): 2971 (m), 2864 (w), 1593 (w), 1457 (m), 1405 (m), 1386 (w), 1373 (w), 1364 (m), 1306 (w), 1258 (w), 1239 (m), 1202 (w), 1163 (m), 1130 (s), 1071 (w), 1031 (w), 998 (m), 940 (vs, $\nu_{Os=O}$), 902 (w), 866 (s), 859 (s), 831 (m), 773 (m), 762 (m), 739 (s), 719 (vs), 699 (s), 688 (s). UV-Vis: λ_{max} = 580 nm (sh, ε = 450 L mol^{-1} cm^{-1}), 425 (1950), 330 (5500), 275 (5800). Anal. Calcd for $C_{26}H_{37}NO_4Os$: C, 50.55; H, 6.04; N, 2.27. Found: C, 50.23; H, 5.97; N, 2.18.

Ethylene glycol dianthranilate, $C_2H_4(O_2CC_6H_4$-2-$NH_2)_2$. Into a 250 mL round-bottom flask are added 1.11 g ethylene glycol (0.0179 mol), 6.28 g isatoic anhydride (0.0385 mol, 2.15 equiv.), 0.95 g 4-dimethylaminopyridine (0.078 mol, 0.4 equiv.), 100 mL chloroform, and a magnetic stirbar. The mixture is refluxed, with stirring, for 25 h. After letting the reaction mixture cool to room temperature, it is poured into a separatory funnel and washed with 100 mL 10% aqueous citric acid. The citric acid layer is washed with 20 mL $CHCl_3$, which is combined with the original chloroform layer, washed with 100 mL water, and dried over magnesium sulfate. After removing the $MgSO_4$ by gravity filtration, the chloroform is removed on a rotary evaporator, leaving a colorless oil which slowly solidifies to a waxy solid. The solid is slurried in 25 mL CH_3OH and suction filtered. The solid is washed with 2 × 10 mL methanol and air-dried 20 min. After the filtrate stands for 3 d, a second crop is deposited, which is isolated by suction filtration, washing with 5 mL methanol, and air-drying as above. The combined yield is 4.07 g (76%). Mp = 102.0–102.8 °C (lit. mp 125–126 °C;[12] 126 °C (ref. 13)). ^{1}H NMR ($CDCl_3$): δ 4.60 (s, 4H, OCH_2CH_2O), 5.58 (br s, 4H, NH_2), 6.64 (t, 8 Hz, 2H, H-5) 6.66 (d, 8 Hz, 2H, H-3), 7.27 (t, 8 Hz, 2H, H-4), 7.89 (d, 8 Hz, 2H, H-6). ^{13}C{^{1}H} NMR ($CDCl_3$): δ 62.37 (O*C*H$_2$*C*H$_2$O), 110.63, 116.57, 116.88, 131.55, 134.49, 150.72, 167.99 (*C*=O). IR (cm^{-1}): 3452 (s, ν_{NH}), 3358 (s, ν_{NH}), 2972 (w), 1684 (vs, $\nu_{C=O}$), 1616 (s), 1591 (m), 1565 (s), 1487 (m), 1458 (m), 1450 (m), 1331 (s), 1295 (m), 1288 (m), 1237 (vs), 1156 (vs), 1096 (m), 1061 (m), 1034 (w), 982 (w), 857 (s), 795 (w), 748 (vs), 700 (s), 663 (s). Anal. Calcd for $C_{16}H_{16}N_2O_4$: C, 63.99; H, 5.37; N, 9.33. Found: C, 64.28; H, 5.40; N, 9.54.

1,2-Ethanediylbis-*N*-(2-hydroxy-3,5-di-*tert*-butylphenyl)anthranilate ($EganH_4$). Into a 20 mL screwcap vial is added 0.4986 g ethylene glycol dianthranilate (1.660 mmol), 0.8032 g 3,5-di-*tert*-butylcatechol (3.613 mmol, 2.2 equiv.), 0.1272 g benzoic acid (1.04 mmol), and a small stirbar. The vial is capped securely and heated in a silicone oil bath maintained at 165 °C for 2 d. The reaction mixture is allowed to cool to room temperature and dissolved in CH_2Cl_2 so the material can be removed from the vial. The solvent is removed on the rotary evaporator, leaving an orange oil, which is dissolved in hexane. After standing 4 h at room temperature, the precipitated solid is suction filtered, washed with 2 × 7 mL hexane, and air-dried 20 min. A second crop is isolated in a similar manner from the filtrate after it partially evaporates; the combined yield is 0.6956 g (59%). Mp = 172.8–173.9 °C. ^{1}H NMR ($CDCl_3$): δ 1.28, 1.45 (s, 18H ea., ^{t}Bu), 4.71 (s, 4H, OCH_2CH_2O), 6.07 (s, 2H, O*H*), 6.53 (d, 8 Hz, 2H, anthranilate H-3), 6.75 (t, 8 Hz, 2H, anthranilate H-5), 7.03 (d, 2 Hz, 2H, aminophenol Ar*H*), 7.26 (d, 2 Hz, 2H, aminophenol Ar*H*), 7.29 (t, 8 Hz, 2H, anthranilate H-4), 8.03 (d, 8 Hz, 2H, anthranilate H-6), 8.81 (br s, 2H, N*H*). ^{13}C{^{1}H} NMR ($CDCl_3$): δ 29.86, 31.93 (C[*C*H$_3$]$_3$), 34.72, 35.39 (*C*[CH$_3$]$_3$), 62.77 (O*C*H$_2$*C*H$_2$O), 112.02, 114.89, 117.75, 122.71, 122.82, 126.45, 131.75, 135.17, 135.90, 142.75, 149.66, 151.08, 168.59 (*C*=O). IR (cm^{-1}): 3476 (m, ν_{OH}), 3324 (m, ν_{NH}), 3000 (w), 2958 (m), 2904 (w), 2867 (w), 1694 (vs, $\nu_{C=O}$), 1604 (m), 1578 (s), 1504 (m), 1478 (s), 1454 (s), 1446 (s), 1424 (m), 1406 (m), 1394 (w), 1372 (w), 1282 (m), 1252 (s), 1228 (vs), 1197 (s), 1167 (s), 1161 (s), 1153 (s), 1142 (s), 1118 (w), 1080 (s), 1048 (w), 1024 (w), 972 (w), 930 (w), 912 (w), 898 (w), 883 (w), 856 (w), 824 (w), 811 (w), 797 (w), 86 (w), 753 (vs), 702 (s), 669 (m). Anal. Calcd for $C_{44}H_{56}N_2O_6$: C, 74.55; H, 7.96; N, 3.95. Found: C, 74.76; H, 8.13; N, 3.92.

(Egan)OsO. Into a 100 mL round-bottom flask is weighed 242.7 mg $EganH_4$ (0.342 mmol) and 159.6 mg OsO$(OCH_2CH_2O)_2$ (0.489 mmol, 1.43 equiv.). To the flask is added 24 mL EtOAc and a stirbar. The flask is then capped with a water-cooled condenser and the reaction mixture is refluxed for 24 h. After cooling to room temperature, the EtOAc is removed on the rotary evaporator and the residue dissolved in $CHCl_3$. The $CHCl_3$ solution is filtered through a plug of silica gel, eluting the dark red-brown band (R_f = 0.42) until the color fades and begins to look more purple. The eluate is stripped down on the rotary evaporator and the residue slurried in CH_3OH. After standing 30 min, the mixture is suction filtered

and the solid washed with 5 mL CH_3OH, then air-dried 20 min to furnish 114.5 mg (Egan)OsO (37%). ^{1}H NMR ($CDCl_3$): δ 0.93, 1.14 (s, 18H ea., ^{t}Bu), 2.79, 4.31 (m, 2H ea., OC*HH*′C*HH*′O), 6.29, 6.58 (d, 2 Hz, 2H ea., amidophenoxide Ar*H*), 7.49 (td, 8, 1.0 Hz, 2H, anthranilate H-5), 7.54 (dd, 8, 1.0 Hz, 2H, anthranilate H-3), 7.80 (td, 8, 1.3 Hz, 2H, anthranilate H-4), 7.90 (dd, 8, 1.3 Hz, 2H, anthranilate H-6). ^{13}C{^{1}H} NMR ($CDCl_3$): δ 29.53, 31.85 (C[*C*H$_3$]$_3$), 34.36, 34.40 (*C*[CH$_3$]$_3$), 62.44 (O*C*H$_2$*C*H$_2$O), 110.44, 120.02, 128.27, 130.33, 131.51, 132.01, 133.26, 135.72, 146.07, 148.70, 149.88, 166.68, 166.75. IR (ATR, cm^{-1}): 3077 (w), 2949 (m), 2904 (w), 2865 (w), 1728 (vs, $\nu_{C=O}$), 1597 (m), 1575 (w), 1477 (m), 1449 (m), 1408 (m), 1362 (m), 1318 (w), 1295 (m), 1284 (s), 1266 (m), 1246 (s), 1232 (s), 1219 (s), 1203 (m), 1168 (w), 1159 (w), 1133 (w), 1117 (s), 1093 (m), 1053 (w), 1041 (w), 1028 (w), 998 (s), 959 (w), 937 (m), 919 (vs, $\nu_{Os=O}$), 902 (s), 876 (m), 865 (s), 845 (w), 831 (m), 785 (m), 776 (w), 762 (m), 750 (w), 733 (vs), 710 (m), 693 (m), 667 (m), 657 (s). UV-vis (CH_2Cl_2): λ_{max} 451 nm (ε = 8200 mol^{-1} L^{-1} cm^{-1}), 362 (11 200), 326 (10 300). Anal. Calcd for $C_{44}H_{52}N_2O_7Os$: C, 58.00; H, 5.75; N, 3.07. Found: C, 57.86; H, 6.00; N, 3.12.

Electrochemistry

Cyclic voltammetry was performed using an Autolab potentiostat (PGSTAT 128N), with glassy carbon working and counter electrodes and a silver/silver chloride reference electrode. The electrodes were connected to the potentiostat through electrical conduits in the drybox wall. Samples were approximately 1 mM in CH_2Cl_2 with 0.1 M Bu_4NPF_6 as the electrolyte. Scans were run at 60 mV s^{-1}, except for (Egan)OsO, which was scanned at 100 mV s^{-1}. Potentials were referenced to ferrocene/ferrocenium at 0 V (ref. 14) with the reference potential established by spiking the test solution with a small amount of ferrocene or decamethylferrocene (E° = –0.565 V *vs.* Cp_2Fe^+/Cp_2Fe in CH_2Cl_2 [15]).

Computational methods

Calculations were performed on compounds with all methyl and *tert*-butyl groups replaced by hydrogen atoms. Geometries were optimized using hybrid density functional theory (B3LYP, SDD basis set for osmium and a 6-31G* basis set for all other atoms), using the Gaussian09 suite of programs,[16] and were confirmed as minima by calculation of vibrational frequencies. Plots of calculated Kohn–Sham orbitals were generated using Gaussview (v. 6.0.16) with an isovalue of 0.04.

X-ray crystallography

Crystals of (^{H}ap)$_2$Os(OCH$_2$CH$_2$O)·0.5 C_6H_{14} were obtained by slow evaporation of a hexane solution of the complex. The deuterodichloromethane solvate of (^{H}ap)$_2$OsCl$_2$ was grown by liquid diffusion of pentane into a solution of the complex in CD_2Cl_2, while the $CDCl_3$ solvate crystallized from a reaction mixture in that solvent. Crystals of (^{H}ap)OsO(pin) were deposited upon diffusion of acetonitrile vapor into chloroform, while crystals of $C_2H_4(O_2CC_6H_4$-2-$NH_2)_2$ formed slowly from a methanol solution of the compound. (Egan)OsO was crystallized by vapor diffusion of methanol into benzene.

Crystals were placed in inert oil before transferring to the N_2 cold stream of a Bruker Apex II CCD diffractometer. Data were reduced, correcting for absorption, using the program SADABS. Calculations used SHELXTL (Bruker AXS),[17] with scattering factors and anomalous dispersion terms taken from the literature.[18] Further details about the structures are in Tables 1 and 2.

Table 1 Summary of crystal data

	(^{H}ap)$_2$Os(OCH$_2$CH$_2$O)·0.5 C_6H_{14}	(^{H}ap)$_2$OsCl$_2$·CD_2Cl_2	(^{H}ap)$_2$OsCl$_2$·$CDCl_3$	(^{H}ap)OsO(pin)	$C_2H_4(O_2CC_6H_4$-2-$NH_2)_2$	(Egan)OsO
Molecular formula	$C_{45}H_{61}N_2O_4Os$	$C_{41}H_{50}D_2Cl_4N_2O_2Os$	$C_{41}H_{50}DCl_5N_2O_2Os$	$C_{26}H_{37}NO_4Os$	$C_{16}H_{16}N_2O_4$	$C_{44}H_{52}N_2O_7Os$
Formula weight	884.15	983.86	972.29	617.76	300.31	911.07
T/K	120(2)	120(2)	120(2)	120(2)	120(2)	120(2)
Crystal system	Triclinic	Orthorhombic	Orthorhombic	Monoclinic	Monoclinic	Triclinic
Space group	$P\bar{1}$	$Fdd2$	$Fdd2$	$P2_1/n$	$C2/c$	$P\bar{1}$
λ/Å	0.71073 (Mo Kα)	0.71073 (Mo Kα)	0.71073 (Mo Kα)	0.71073 (Mo Kα)	0.71073 (Mo Kα)	0.71073 (Mo Kα)
Total data collected	29 521	47 083	33 267	35 684	10 143	66 041
No. of indep reflns.	10 122	5202	5294	7245	1736	12 637
R_{int}	0.0396	0.0487	0.0238	0.0250	0.0481	0.0210
Obsd refls [$I > 2\sigma(I)$]	9073	4719	5033	6459	1266	11 999
a/Å	12.2153(6)	16.7630(14)	16.8082(7)	10.1408(4)	13.142(3)	13.0153(6)
b/Å	13.1499(7)	40.360(4)	40.829(2)	16.5112(6)	11.273(3)	13.1218(7)
c/Å	13.2104(7)	12.3474(14)	12.5096(7)	15.0329(5)	9.569(2)	14.0466(6)
α/°	103.1226(17)	90	90	90	90	105.229(2)
β/°	91.7443(16)	90	90	96.6940(10)	102.307(5)	104.4965(19)
γ/°	97.8182(17)	90	90	90	90	108.180(2)
V/Å^3	2043.22(18)	8353.7(15)	8584.8(8)	2499.90(16)	1385.1(6)	2049.60(17)
Z	2	8	8	4	4	2
μ/mm^{-1}	3.164	3.344	3.317	5.132	0.105	3.162
Crystal size/mm	0.12 × 0.12 × 0.06	0.09 × 0.09 × 0.09	0.23 × 0.20 × 0.19	0.32 × 0.30 × 0.12	0.22 × 0.12 × 0.12	0.21 × 0.13 × 0.12
No. refined params	543	235	329	437	132	695
$R1$, w$R2$ [$I > 2\sigma(I)$]	$R1$ = 0.0357	$R1$ = 0.0256	$R1$ = 0.0140	$R1$ = 0.0195	$R1$ = 0.0385	$R1$ = 0.0140
	w$R2$ = 0.0672	w$R2$ = 0.0472	w$R2$ = 0.0322	w$R2$ = 0.0422	w$R2$ = 0.0951	w$R2$ = 0.0332
$R1$, w$R2$ [all data]	$R1$ = 0.0438	$R1$ = 0.0322	$R1$ = 0.0156	$R1$ = 0.0242	$R1$ = 0.0593	$R1$ = 0.0156
	w$R2$ = 0.0692	w$R2$ = 0.0488	w$R2$ = 0.0327	w$R2$ = 0.0436	w$R2$ = 0.1035	w$R2$ = 0.0336
Goodness of fit	1.121	1.057	1.047	1.040	1.074	1.046

Table 2 Selected bond distances, angles, and metrical oxidation states of iminoxolene ligands of structurally characterized compounds. Values given are the average of chemically equivalent measurements (averaged over both solvates for $(^{H}ap)_2OsCl_2$ and over the pseudo-twofold axes in $(^{H}ap)_2Os(OCH_2CH_2O)$ and (Egan)OsO). DFT MOS calculations used ligands in which *tert*-butyl and methyl groups were replaced by hydrogen

	$(^{H}ap)_2Os(OCH_2CH_2O)$	$(^{H}ap)_2OsCl_2$	$(^{H}ap)OsO(pin)$	(Egan)OsO
Bond distances/Å				
Os–O			1.6825(16)	1.6951(9)
Os–O1	1.975(5)	2.008(3)	1.9448(14)	1.929(5)
Os–N1	1.972(4)	1.958(4)	1.9002(17)	1.9286(16)
Os–O3	1.946(8)		1.8945(14)	
Os–O4			1.8884(14)	
Os–Cl		2.3626(10)		
O1–C11	1.333(5)	1.303(5)	1.359(2)	1.3674(14)
N1–C12	1.383(5)	1.353(6)	1.412(2)	1.406(3)
C11–C12	1.407(5)	1.438(5)	1.384(3)	1.386(3)
C12–C13	1.408(8)	1.417(6)	1.386(3)	1.389(3)
C13–C14	1.379(5)	1.358(7)	1.383(3)	1.3881(17)
C14–C15	1.417(5)	1.442(5)	1.398(3)	1.401(2)
C15–C16	1.377(6)	1.366(5)	1.393(3)	1.3938(17)
C11–C16	1.418(5)	1.428(5)	1.397(3)	1.397(3)
Metrical Oxidation State (MOS)[19]	−1.47(10)	−0.94(8)	−1.97(14)	−1.98(12)
MOS from DFT calculations	−1.45(7)	−1.05(6)	−1.96(8)	−1.95(7)
Bond angles/°				
O1–Os–N1	79.33(11)	78.80(12)	81.14(6)	80.66(17)
O3–Os–O4	79.59(12)		82.11(6)	
Cl1–Os–Cl1A		89.5(3)		
O–Os–O1			102.49(7)	108.67(16)
O–Os–N1			110.63(8)	110.66(6)
O–Os–O3			107.70(7)	
O–Os–O4			118.59(7)	
τ[20]			0.32	0.07

Results

Preparation of osmium bis(*N*-arylamidophenoxide) complexes

The osmium(VI) mono-oxo complex $OsO(OCH_2CH_2O)_2$, prepared from osmium tetroxide and ethylene glycol,[11] reacts with substituted *N*-aryl-2-amino-4,6-di-*tert*-butylphenols ($^{R}apH_2$) in acetone or chloroform to give bis(amidophenoxide) oxoosmium(VI) complexes $(^{R}ap)_2OsO$ (eqn (1)). The complexes are sparingly soluble in all organic solvents, with maximal solubility in chlorinated solvents, and so can be isolated by filtration from the reaction mixtures. They can be purified, if necessary, by Soxhlet extraction with dichloromethane. Reactions are generally complete overnight, except for the *p*-CF_3 derivative, which reacts much more slowly. ^{1}H NMR spectra of the compounds show resonances at diamagnetic chemical shifts, with the *ortho* and *meta* (but not *para*) resonances of the *N*-aryl groups somewhat broadened, indicating that the top and bottom of the amidophenoxide ligands are inequivalent and that rotation is slow ($k \approx 20\ s^{-1}$).

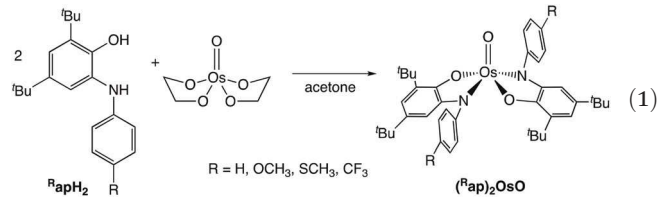

(1)

Hindered rotation in ^{R}ap complexes has been observed previously.[21] The compounds show small amounts of a second species by NMR, tentatively assigned as the *cis* isomer. The isomer ratio varies depending on the aryl substituent, with the methoxyphenyl compound $(^{MeO}ap)_2OsO$ showing the largest amount of the minor isomer (15%). The presence of a terminal oxo group is confirmed by the observation of a very strong band in the IR in the range of 904–906 cm^{-1}.

If the reaction of $^{H}apH_2$ with $OsO(OCH_2CH_2O)_2$ is carried out in dichloromethane, then $(^{H}ap)_2OsO$ is not formed, and the major product is the ethylene glycolate complex $(^{H}ap)_2Os(OCH_2CH_2O)$ (eqn (2)). This is analogous to the reaction of the bis(aminophenol) 2,2′-biphenylbis(3,5-di-*tert*-butyl-2-hydroxyphenylamine) ($ClipH_4$).[5] The chelated complex (Clip)Os(OCH_2CH_2O) forms only the *cis*-β stereoisomer, but the broadened ^{1}H NMR of $(^{H}ap)_2Os(OCH_2CH_2O)$ at room temperature indicates that the latter compound is a mixture of stereoisomers. Variable-temperature NMR spectra indicate that two stereoisomers are present in a 9 : 1 ratio at low temperature (<–60 °C). In the solid state, the complex shows a *cis*-α geometry with the amidophenoxide nitrogens mutually trans (Fig. 2).

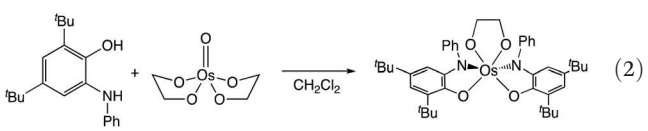

(2)

Heating the ethylene glycolate complex or the oxo complex with chlorotrimethylsilane affords the dichloride complex $(^{H}ap)_2OsCl_2$ (eqn (3)). The compound can also be prepared by treatment of $(^{H}ap)_2OsO$ with phosphorus pentachloride. The

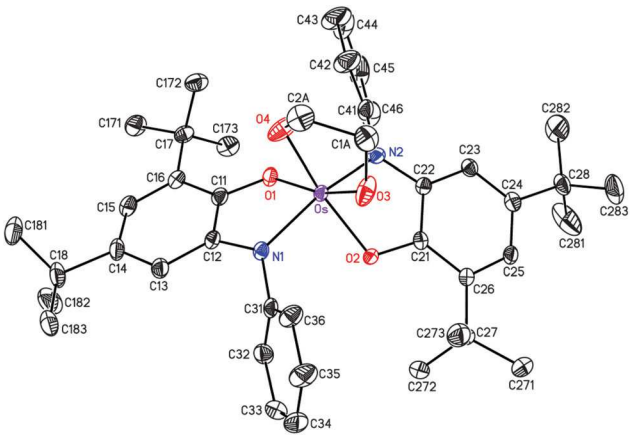

Fig. 2 Thermal ellipsoid plot of $(^{H}ap)_2Os(OCH_2CH_2O)\cdot 0.5C_6H_{14}$, with hydrogen atoms and lattice solvent omitted for clarity. Only the major orientation of the disordered ethylene bridge and *tert*-butyl group at C18 are shown.

dichloride exists as almost entirely (>95%) one stereoisomer in CD_2Cl_2, but as a 61 : 17 : 22 mixture of the two *cis*-α and *cis*-β isomers in C_6D_6 (Fig. S1†). The rate of interconversion of the stereoisomers is much slower for the dichloride complex than for the ethylene glycolate, presumably because the smaller bite angle of the ethylene glycolate (Table 2) accelerates the trigonal twisting pathway.[22] The major stereoisomer is assigned to the *cis*-α isomer with the amidophenoxide oxygens mutually trans, as that is what is observed in the solid state (Fig. 3). The preference for the opposite *cis*-α isomer compared to the ethylene glycolate is attributed to a trans influence: the most strongly donating imino nitrogen prefers to be trans to the most weakly donating chloride, whereas the strongly donating glycolate oxygens prefer to be trans to the oxygen end of the amidophenoxides.

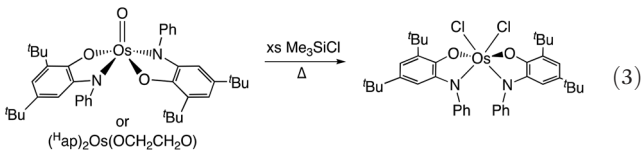

(3)

The first step in the reactions of $^{H}apH_2$ with $OsO(OCH_2CH_2O)_2$ in both acetone and dichloromethane appears to be displacement of ethylene glycol, as the monooxo-monoglycolate complex $(^{H}ap)OsO(OCH_2CH_2O)$ can be observed *in situ* by ^1H NMR in the early stages of the reaction. The pinacolate analogue of this compound, $(^{H}ap)OsO(pin)$, has been isolated and fully characterized. It is prepared by initial treatment of osmium tetroxide with 2,3-dimethyl-2-butene to form the pinacolate ester $(pin)OsO(\mu\text{-}O)_2OsO(pin)$,[11] followed by treatment with the aminophenol $^{H}apH_2$ (eqn (4)).

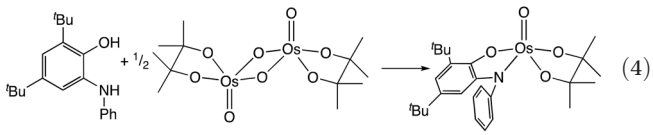

(4)

The solid state structure of the compound (Fig. 4) confirms the presence of a distorted square pyramidal structure with a

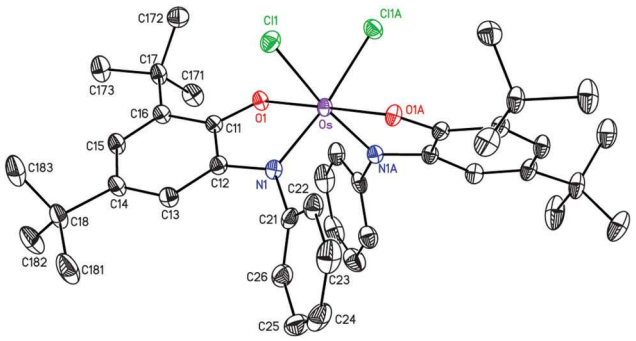

Fig. 3 Thermal ellipsoid plot of $(^{H}ap)_2OsCl_2\cdot CD_2Cl_2$, with hydrogen atoms and lattice solvent omitted for clarity.

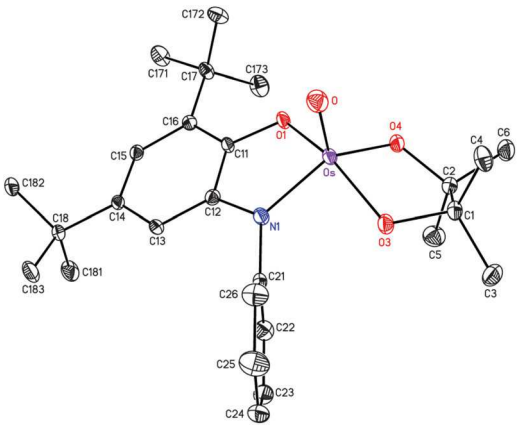

Fig. 4 Thermal ellipsoid plot of $(^{H}ap)OsO(pin)$, with hydrogen atoms omitted for clarity.

short osmium-oxo distance (Table 2), similar to that of other osmium mono-oxo glycolates with amide donors.[23] The *ortho* and *meta* positions of the *N*-phenyl group show broadened resonances in the ^1H and ^{13}C NMR spectra, indicative of slow rotation about the carbon–nitrogen bond, as in $(^{R}ap)_2OsO$. The pinacolate ligand in $(^{H}ap)OsO(pin)$ is tightly bonded to osmium; for example, it is not displaced by $^{H}apH_2$ even on heating for several days at 70 °C. The much lower reactivity of pinacolate compared to ethylene glycolate is presumably steric in origin.

Preparation of a trans-spanning chelating bis(aminophenol) and its oxoosmium complex

While simple aminophenols readily form oxobis(amidophenoxide) complexes with osmium, chelating bis-aminophenols do not. For example, reaction of $OsO(OCH_2CH_2O)_2$ with the 2,2′-biphenylenediyl-bridged bis-aminophenol $ClipH_4$ affords only $(Clip)Os(OCH_2CH_2O)$.[5] We reasoned that this might be due to the preference of $(^{R}ap)_2OsO$ to adopt a *trans* geometry incompatible with a tetradentate ligand with a short tether between nitrogen atoms. Alternatively, the strongly pyramidalized geometry at osmium in an oxo complex (the average O–Os–L angle in $(^{H}ap)OsO(pin)$ is 110°) might be incompatible

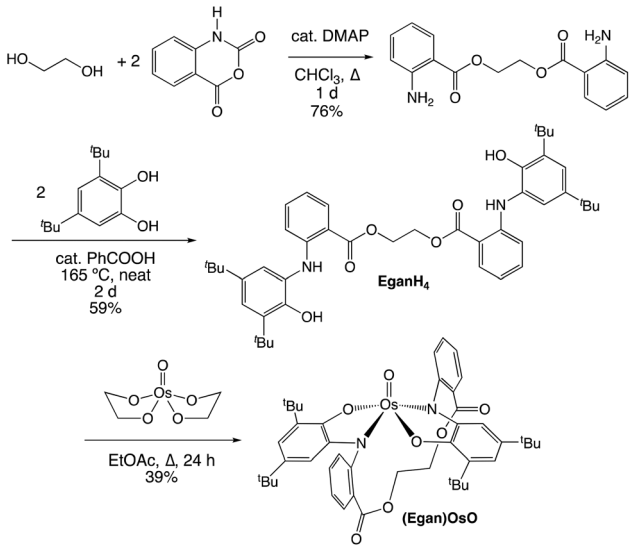

Scheme 1 Preparation and metalation of the bis-aminophenol $EganH_4$.

with existing tetradentate bis-aminophenols, which, when occupying a square set of coordination sites, are observed to be planar[24,25] or twisted.[5,26,27]

We therefore set out to prepare the $EganH_4$ ligand (Scheme 1) based on an ethylene glycol dianthranilate core, which molecular models and DFT calculations suggested would be compatible with a *trans*, highly pyramidalized geometry. The dianthranilate ester had been reported previously as the product of NaOH-catalyzed reaction of ethylene glycol with isatoic anhydride[12] or of hydrogenation of ethylene glycol bis(*o*-nitrobenzoate).[13] We find that 4-(dimethylamino)pyridine (DMAP) is an effective catalyst for anthraniloylation[28] of ethylene glycol by isatoic anhydride, affording the dianthranilate (characterized crystallographically, Fig. S2†) in a single step in good yield. The condensation of this diamine with 3,5-di-*tert*-butylcatechol is not catalyzed by triethylamine at any temperature, but slow conversion is observed in toluene at 110° in the presence of a carboxylic acid catalyst. Practical rates are achieved on heating a neat mixture of dianthranilate, di-*tert*-butylcatechol, and benzoic acid at 165 °C. Previously reported condensations of 3,5-di-*tert*-butylcatechol with anilines with electron-withdrawing *ortho* substituents also require forcing conditions.[29]

Metalation of $EganH_4$ with $OsO(OCH_2CH_2O)_2$ is much slower than reactions of simple arylaminophenols, but is accomplished in moderate yield after heating for a day in ethyl acetate or benzene. Unlike $(^{R}ap)_2OsO$, (Egan)OsO has good solubility in most organic solvents, and is isolated from the complex reaction mixture by initial filtration through a plug of silica gel, followed by precipitation with methanol.

The monomeric square pyramidal structure with trans amidophenoxides is confirmed by X-ray crystallography (Fig. 5), which shows that the molecule possesses a short Os=O multiple bond (1.6951(9) Å) and a nearly perfect noncrystallographic twofold axis of symmetry. The C_2 symmetry of the

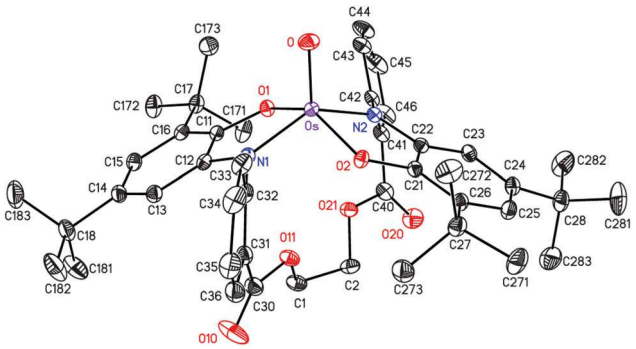

Fig. 5 Thermal ellipsoid plot of (Egan)OsO, with hydrogen atoms omitted for clarity.

complex is observed in solution as well, judging from its ^{1}H and ^{13}C NMR spectra. The ester groups adopt a typical *s-cis* conformation and appear to be unstrained, judging from the normal carbonyl stretching frequency observed in the IR (1728 cm^{-1}, compare ethylene glycol dibenzoate[30] at 1726 cm^{-1}). This frequency is significantly blue-shifted compared to the free ligand (1694 cm^{-1}), because the amino group is metalated and the ligand conformation requires the iminoxolene plane to be nearly perpendicular to the phenyl group (average angle between planes = 59°). This minimizes the electron donation of the amino group and eliminates the hydrogen bonding that together lower the stretching frequency in the free ligand.

Optical spectroscopy and electrochemistry

The oxo-iminoxolene complexes show a series of moderately intense transitions in the near-UV and blue region of the visible spectrum (Fig. 6). The appearance of the spectrum of $(^{H}ap)_2OsO$ is similar to that of the isoelectronic complex

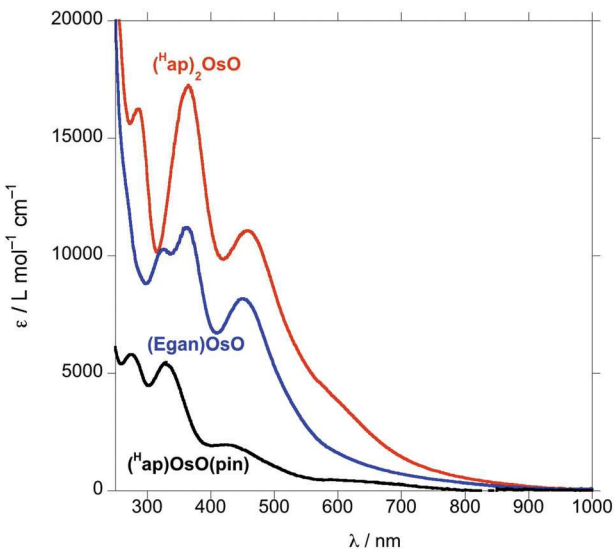

Fig. 6 UV-visible spectra (in CH_2Cl_2) of $(^{H}ap)_2OsO$ (red trace), (Egan)OsO (blue trace) and $(^{H}ap)OsO(pin)$ (black trace).

with *o*-benzenediamide-derived ligands, $(PhNC_6H_4NH)_2OsO$, though the low-energy features of the benzenediamide complex are red-shifted by about 80 nm relative to those of the amidophenoxide complex.[31] The similarity of the constrained complex (Egan)OsO to the unconstrained complexes indicates that the tether does not significantly perturb the electronic structure of the compounds. The mono-iminoxolene complex (^{H}ap)OsO(pin) also shows similar spectral features, though the intensities of all bands are lower and the most intense bands are blue-shifted by about 35 nm. Substituents have little effect on the electronic spectra of (^{R}ap)$_2$OsO (Fig. S3†), with small variations in peak position that are not well correlated with the nature of the substituent (for example, the compound with R = H absorbs to the blue of compounds with either electron-donating or -withdrawing substituents).

The spectra of the octahedral complexes (^{H}ap)$_2OsCl_2$ and (^{H}ap)$_2$Os(OCH_2CH_2O) are quite different from the oxo complexes, but very similar to each other (Fig. S4†). They are dominated by intense, relatively narrow absorptions in the visible region, and show weak, broad absorptions in the near-IR. These features are very similar to the analogous (Clip)Os complexes,[5] with the weak bands in the near-IR attributed to d → Os-iminoxolene π* transitions and the strong bands in the visible assigned as Os-iminoxolene π → π* transitions.

Electrochemically, the (^{R}ap)$_2$OsO complexes are generally too insoluble to be studied by cyclic voltammetry. The chelated complex (Egan)OsO shows only irreversible oxidations at >0.7 V *vs.* Fc^+/Fc, and one reversible reduction at −1.26 V (Fig. S5†). The mono-iminoxolene complex (^{H}ap)$_2$OsO(pin) is similar (Fig. S6†). The octahedral complexes (^{H}ap)$_2$Os(OCH_2CH_2O) and (^{H}ap)$_2OsCl_2$ show both reversible oxidations and reversible reductions, with the latter shifted about 350 mV to higher potential compared to the former (Fig. S7†). The cyclic voltammograms of these two compounds are very similar to the *cis*-β-(Clip) analogues,[5] except that the second reduction of (^{H}ap)$_2OsCl_2$ is irreversible while *cis*-β-(Clip)$OsCl_2$ has two reversible reductions.

Discussion

Structure and bonding as a function of ancillary ligand

The most striking aspect of the structures of the iminoxolene complexes described here is the marked variation of the intraligand distances in the iminoxolenes with the nature of the ancillary ligands bonded to osmium. These intraligand distances reflect the electron density in the iminoxolene redox-active orbital. Inspection of this orbital (Fig. 1) shows, for example, that it is C–O and C–N antibonding, so as the electron density in this orbital increases, these bonds will be correspondingly lengthened. As the donor strength of the ancillary ligands increase from dichloride to ethylene glycolate to oxo, there is a corresponding steady increase of the lengths of the iminoxolene C–O bond and C–N bond, with an overall change of ∼0.06 Å in each bond length.

These changes (and other, smaller, changes in the C–C bond lengths of the iminoxolene) can be combined to give an apparent or "metrical" oxidation state (MOS) that reports the effective number of electrons on the ligand in the redox-active orbital.[19] In the five-coordinate oxo compounds (^{H}ap)OsO(pin) (MOS = −1.97(14)) and (Egan)OsO (MOS = −1.98(12)), the observed MOS values are within experimental error of −2, indicating an iminoxolene whose structure is characteristic of a fully reduced ligand that engages in little π bonding with the metal. Given the geometry of these complexes, π bonding from the iminoxolene would have to compete with π bonding to the oxo ligand, and the oxo ligand apparently wins this competition. A similar effect is observed, for example, in *cis*-(Clip)Mo(O)(3,5-lutidine),[6] where the geometry of the iminoxolene relative to the oxo ligand dramatically affects the π bonding. The iminoxolene *cis* to the oxo must compete with it and so does not display noticeable π bonding (MOS = −2.00(9)), while the iminoxolene trans to the oxo, which can interact with the d orbital that is δ with respect to the oxo ligand and thus does not compete with it, is appreciably π donating (MOS = −1.34(12)).

When the osmium complexes have less strongly π donating ancillary ligands, the degree of π bonding exhibited by the iminoxolenes increases. Chloride is a negligible π donor, and the *cis* geometry in (^{H}ap)$_2OsCl_2$ allows the formation of two metal-iminoxolene π bonds. The observed MOS of −0.94(8) can thus be interpreted as indicating a nearly equal-sharing covalent interaction between the ligand RAOs and the Os dπ orbitals, resulting in a decrease in electron density on the ligand in the occupied orbitals due to delocalization of the electron onto the metal. This is consistent with the observations of other osmium iminoxolenes, where a π bond order of one is expected to result in an MOS of about −1.16(5).[5]

Ethylene glycolate is a stronger π donor than chloride but weaker than oxo. It therefore competes better with the iminoxolene for π bonding to osmium than the dichloride but worse than the oxo, so the MOS in the ethylene glycolate complex, −1.47(10), is intermediate between the other two complexes. The three compounds thus lie on a continuum of π bonding, and can be viewed, for example, as containing a formally Os(VI) center with increasingly π-donating amidophenoxides as the ancillary ligands change from oxo to glycolate to dichloride. An alternative ionic model that attempts to sort the ligands into amidophenoxide *vs.* iminosemiquinone is more cumbersome and less illuminating. Based on the structural data, one would be obliged to classify the compounds as being Os(VI)-bis(amidophenoxide) (oxo), Os(V)-monoamidophenoxide-monoiminosemiquinone (glycolate), and Os(IV)-bis(iminosemiquinone) (dichloride). This has the particularly unfortunate consequence that the electronic structure in the glycolate and the dichloride would be made to appear to be qualitatively different, which flies in the face of the obvious similarities of their optical spectra.

Anisotropy of metal-oxo π bonding in oxo-iminoxolene complexes

Just because the extent of osmium-iminoxolene π bonding in the oxo-iminoxolene complexes is too small to have a notice-

able structural impact does not imply that it is entirely absent. The effect of π bonding can be discerned through an analysis of the bonding and optical spectroscopy of, for example, $(^{H}ap)_2OsO$ (Fig. 7). In this C_2-symmetric molecule, the ligand RAOs form one *A*- and one *B*-symmetry combination, which predominate in the HOMO−1 and HOMO, respectively. Both of the metal-oxo π* orbitals are of *B* symmetry, which means that only one interacts with the iminoxolene RAOs. This effectively pushes up the LUMO+1 in energy, as it gains some Os-iminoxolene π* character, relative to the LUMO, which remains purely Os-oxo π*. (The energies of the HOMO and HOMO−1 are also split by differential interactions with the osmium, but the *A*-symmetry orbital can π donate into the osmium-oxo σ* orbital due to the highly pyramidalized geometry, so the calculated energy difference is smaller, with the *A*-symmetry orbital actually calculated to be lower in energy than the *B*-symmetry orbital.) The split between the LUMO and LUMO+1 is calculated to be 0.31 eV (2500 cm^{-1}).

The effect of this splitting can be seen in the optical spectra of the oxo-iminoxolene complexes. With the aid of time-dependent DFT (TDDFT) calculations, the low-energy shoulder in the spectrum of $(^{H}ap)_2OsO$ at 580 nm (calc. 596 nm) can be assigned to the (HOMO−1) → LUMO transition, while the more intense peak at 458 nm (calc. 499 nm) is assigned to the (HOMO−1) → (LUMO+1) transition. (The corresponding bands originating from the HOMO are calculated to be much lower in intensity and are not observed experimentally.) The splitting between these bands (4600 cm^{-1} exptl., 3300 cm^{-1} calc.) is thus due to the splitting between the two osmium-oxo π* orbitals.

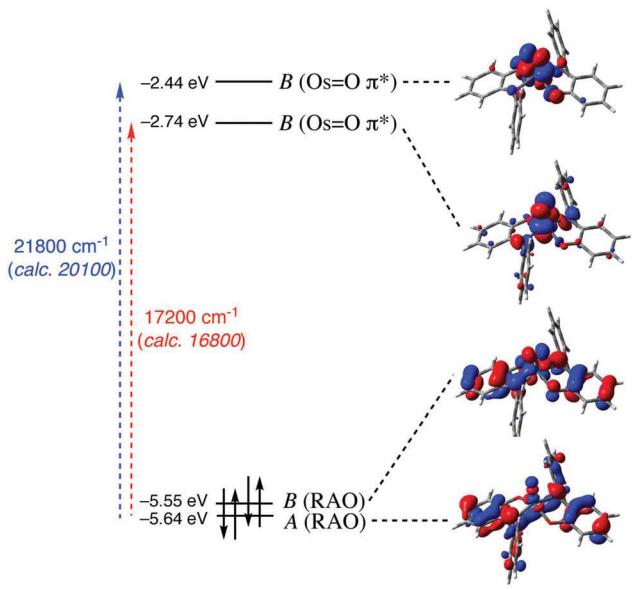

Fig. 7 Molecular orbital diagram of C_2-symmetric $(^{H}ap)_2OsO$, with *tert*-butyl groups replaced by hydrogen. Orbital energies are those calculated for the corresponding Kohn–Sham orbitals (B3LYP, 6-31G*/SDD for Os). Frequencies are for the observed optical transitions (TDDFT calculated frequencies given in parentheses).

The difference in energy between two optical transitions cannot in general be simply translated into orbital energy differences because of differences in electron–electron repulsion in the excited states. In this case, however, the relatively high localization of the donor (on the iminoxolenes) and acceptor (on the osmium-oxo group) orbitals means that these differences are expected to be small[32] and thus the optical excitation differences should translate well into orbital energy differences. An energy difference of ~4000 cm^{-1} (11 kcal mol^{-1}) is modest on the scale of the energy of a π bond (estimated for Mo-iminoxolenes as ~40 kcal mol^{-1},[2] and undoubtedly larger for Os), consistent with the imperceptibility of the change in MOS from the value of −2.00 expected in the absence of π bonding. But such an energy difference is large in chemical terms (a factor of $\sim10^8$ in rate at room temperature). This suggests a chemically significant degree of anisotropy in the metal-oxo bonding in $(^{H}ap)_2OsO$.

The lower-energy Os=O π* orbital is directed between the two iminoxolenes, implying that nucleophiles (such as phosphines) will have a strong preference to attack the oxygen along trajectories that fall between the ligands. In contrast, the presence of a modest degree of oxygen p orbital character perpendicular to this direction in the HOMO indicates that electrophiles (such as Me_3SiCl) will prefer to approach the oxo ligand over the face of the iminoxolene ligands. This anisotropy stands in stark contrast to most monooxo complexes, which have degenerate or nearly degenerate π* orbitals and thus have cylindrically symmetrical bonding. The implications of the electronic anisotropy of the Os=O linkage in $(^{H}ap)_2OsO$ on reactivity and stereoselectivity are currently being explored.

Conclusions

Osmium forms a variety of bis(iminoxolene) complexes of the form $(^{R}ap)_2OsX_2$ (X_2 = O, OCH_2CH_2O, or Cl) from 2-arylamino-4,6-di-*tert*-butylphenols. The bis(aminophenol) $EganH_4$ derived from ethylene glycol dianthranilate forms a square pyramidal oxo complex (Egan)OsO with a trans geometry. The structural and spectroscopic features of these complexes are consistent with a series in which the iminoxolene-osmium π bonding increases as the π donor abilities of the ancillary groups decrease. In particular, the oxo ligand is such a strong π donor that it decisively outcompetes the iminoxolenes for π bonding, so that the $(^{R}ap)_2OsO$ compounds can be reasonably assigned as containing fully reduced amidophenoxide ligands. While the iminoxolene π bonding in these oxo complexes is small, it is not entirely negligible. Optical spectroscopy and DFT calculations indicate that the two Os=O π* orbitals are split in energy by ~4000 cm^{-1} due to differential π donation from the amidophenoxide donor orbitals. The oxo ligand in $(^{R}ap)_2OsO$ is thus electronically anisotropic, with the oxygen p orbital pointing from one iminoxolene to the other contributing preferentially to the HOMO and the p

orbital between the two iminoxolenes contributing preferentially to the LUMO.

Conflicts of interest

There are no conflicts to declare.

Acknowledgements

We thank Dr Allen G. Oliver for his assistance with the X-ray crystallography. This work was supported by the US National Science Foundation (grant CHE-1465104). J. G. thanks the US Department of Education (GAANN grant P200A1320203-14) for a fellowship. S. J. M. thanks the College of Science and the Glynn Family Honors Program at the University of Notre Dame for summer fellowship support.

Notes and references

1 A. I. Poddel'sky, V. K. Cherkasov and G. A. Abakumov, *Coord. Chem. Rev.*, 2009, **253**, 291–324.
2 T. Marshall-Roth and S. N. Brown, *Dalton Trans.*, 2015, **44**, 677–685.
3 R. F. Munhá, R. A. Zarkesh and A. F. Heyduk, *Dalton Trans.*, 2013, **42**, 3751–3766.
4 X. Sun, H. Chun, K. Hildenbrand, E. Bothe, T. Weyhermüller, F. Neese and K. Wieghardt, *Inorg. Chem.*, 2002, **41**, 4295–4303.
5 J. Gianino and S. N. Brown, *Dalton Trans.*, 2020, **49**, 7015–7027.
6 J. A. Kopec, S. Shekar and S. N. Brown, *Inorg. Chem.*, 2012, **51**, 1239–1250.
7 C. A. Lippert, K. I. Hardcastle and J. D. Soper, *Inorg. Chem.*, 2011, **50**, 9864–9878.
8 K. Ley and F. Lober, *FRG Pat*, 1119297, 1961.
9 O. I. Shadyro, V. L. Sorokin, G. A. Ksendzova, G. I. Polozov, S. N. Nikolaeva, N. I. Pavlova, O. V. Savinova and E. I. Boreko, *Pharm. Chem. J.*, 2003, **37**, 399–401.
10 J. Jacquet, P. Chaumont, G. Gontard, M. Orio, H. Vezin, S. Blanchard, M. Desage-El Murr and L. Fensterbank, *Angew. Chem., Int. Ed.*, 2016, **55**, 10712–10716.
11 R. J. Collin, J. Jones and W. P. Griffith, *J. Chem. Soc., Dalton Trans.*, 1974, 1094–1097.
12 R. P. Staiger and E. B. Miller, *J. Org. Chem.*, 1959, **24**, 1214–1219.
13 R. Jacquemain and G. Devillers, *Compt. Rend.*, 1938, **206**, 1305–1307.
14 N. G. Connelly and W. E. Geiger, *Chem. Rev.*, 1996, **96**, 877–910.
15 D. Lionetti, A. J. Medvecz, V. Ugrinova, M. Quiroz-Guzman, B. C. Noll and S. N. Brown, *Inorg. Chem.*, 2010, **49**, 4687–4697.
16 M. J. Frisch, G. W. Trucks, H. B. Schlegel, G. E. Scuseria, M. A. Robb, J. R. Cheeseman, G. Scalmani, V. Barone, B. Mennucci, G. A. Petersson, H. Nakatsuji, M. Caricato, X. Li, H. P. Hratchian, A. F. Izmaylov, J. Bloino, G. Zheng, J. L. Sonnenberg, M. Hada, M. Ehara, K. Toyota, R. Fukuda, J. Hasegawa, M. Ishida, T. Nakajima, Y. Honda, O. Kitao, H. Nakai, T. Vreven, J. A. Montgomery Jr., J. E. Peralta, F. Ogliaro, M. Bearpark, J. J. Heyd, E. Brothers, K. N. Kudin, V. N. Staroverov, R. Kobayashi, J. Normand, K. Raghavachari, A. Rendell, J. C. Burant, S. S. Iyengar, J. Tomasi, M. Cossi, N. Rega, J. M. Millam, M. Klene, J. E. Knox, J. B. Cross, V. Bakken, C. Adamo, J. Jaramillo, R. Gomperts, R. E. Stratmann, O. Yazyev, A. J. Austin, R. Cammi, C. Pomelli, J. W. Ochterski, R. L. Martin, K. Morokuma, V. G. Zakrzewski, G. A. Voth, P. Salvador, J. J. Dannenberg, S. Dapprich, A. D. Daniels, O. Farkas, J. B. Foresman, J. V. Ortiz, J. Cioslowski and D. J. Fox, *Gaussian 09, Revision A.02*, Gaussian, Inc., Wallingford CT, 2009.
17 G. M. Sheldrick, *Acta Crystallogr., Sect. A: Found. Crystallogr.*, 2008, **64**, 112–122.
18 *International Tables for Crystallography*, ed. A. J. C. Wilson, Kluwer Academic Publishers, Dordrecht, The Netherlands, 1992, vol C.
19 S. N. Brown, *Inorg. Chem.*, 2012, 1251–1260.
20 A. W. Addison, T. N. Rao, J. Reedijk, J. van Rijn and G. C. Verschoor, *J. Chem. Soc., Dalton Trans.*, 1984, 1349–1356.
21 A. N. Erickson and S. N. Brown, *Dalton Trans.*, 2018, **47**, 15583–15595.
22 (*a*) S. S. Eaton, J. R. Hutchison, R. H. Holm and E. L. Muetterties, *J. Am. Chem. Soc.*, 1972, **94**, 6411–6426; (*b*) A. Rodger and B. F. G. Johnson, *Inorg. Chem.*, 1988, **27**, 3061–3062.
23 (*a*) S. Hanessian, P. Meffre, M. Girard, S. Beaudoin, J.-Y. Sancéau and Y. Bennani, *J. Org. Chem.*, 1993, **58**, 1991–1993; (*b*) T. J. Donohoe, R. M. Harris, S. Butterworth, J. N. Burrows, A. Cowley and J. S. Parker, *J. Org. Chem.*, 2006, **71**, 4481–4489.
24 K. S. Min, T. Weyhermüller, E. Bothe and K. Wieghardt, *Inorg. Chem.*, 2004, **43**, 2922–2931.
25 D. D. Swanson, K. M. Conner and S. N. Brown, *Dalton Trans.*, 2017, **46**, 9049–9057.
26 C. Mukherjee, T. Weyhermüller, E. Bothe and P. Chaudhuri, *Inorg. Chem.*, 2008, **47**, 11620–11632.
27 K. M. Conner, A. L. Perugini, M. Malabute and S. N. Brown, *Inorg. Chem.*, 2018, **57**, 3272–3286.
28 (*a*) B. D. Allison, V. K. Phuong, L. C. McAtee, M. Rosen, M. Morton, C. Prendergast, T. Barrett, G. Lagaud, J. Freedman, L. Li, X. Wu, H. Venkatesan, M. Pippel, C. Woods, M. Rizzolio, M. Hack, K. Hoey, X. Deng, C. King, N. P. Shankley and M. H. Rabinowitz, *J. Med. Chem.*, 2006, **49**, 6371–6390; (*b*) A. V. Kurkin, A. A. Bernovskaya and M. A. Yurovskaya, *Tetrahedron: Asymmetry*, 2010, **21**, 2100–2107.
29 (*a*) A. V. Piskunov, I. V. Ershova, M. V. Gulenova, K. I. Pashanova, A. S. Bogomyakov, I. V. Smolyaninov, G. K. Fukin and V. K. Cherkasov, *Russ. Chem. Bull., Int. Ed.*,

2015, **64**, 642–649; (*b*) A. V. Piskunov, K. I. Pashanova, A. S. Bogomyakov, I. V. Smolyaninov, N. T. Berberova and G. K. Fukin, *Polyhedron*, 2016, **119**, 286–292.
30 F. J. Boerio and S. K. Bahl, *Spectrochim. Acta*, 1976, **32A**, 987–1006.
31 S. Samanta, L. Adak, R. Jana, G. Mostafa, H. M. Tuononen, B. C. Ranu and S. Goswami, *Inorg. Chem.*, 2008, **47**, 11062–11070.
32 T. B. Karpishin, M. S. Gebhard, E. I. Solomon and K. N. Raymond, *J. Am. Chem. Soc.*, 1991, **113**, 2977–2984.